

Nonlinear Control of Grid Connected PV Systems With Three Level NPC Inverter

Tahir Khalfallah

Department of Electrical Engineering
University of Tiaret, Tiaret BP 078
14000 Tiaret, Algeria
tahir.commande@gmail.com

Miloudi Abdallah

Department of Electrical Engineering
University of Saida, Saida BP 138
20000 Saida, Algeria
amiloudidz@yahoo.fr

Tahir sofiane

Department of Electrical Engineering
University of Saida, Saida BP 138
20000 Saida, Algeria
amiloudidz@yahoo.fr

Belfedal Cheikh

Department of Electrical Engineering
University of Tiaret, Tiaret BP 078
14000 Tiaret, Algeria
bochradz@yahoo.com

Doumi M'Hamed

Department of Electrical Engineering
University of Bechar, Bechar BP 417,
08000 Bechar, Algeria
doumicanada@gmail.com

Abdel Ghani Aissaoui

Department of Electrical Engineering
University of Bechar, Bechar B.P 417,
08000 Bechar, Algeria
irecom_aissaoui@yahoo.fr

Abstract— this paper presents a control for a three phase three-level neutral point clamped inverter (NPC) for grid connected photovoltaic (PV) system. The maximum power point tracking (MPPT) is capable of extracting maximum power from the photovoltaic (PV) array connected to each DC link voltage level. The MPPT algorithm is solved by Perturb and Observe (P&O) method. The MPPT system is integrated with the DC-link controller so that a DC-DC converter is not needed and the output shows accurate and fast response. We seek the achievement of three control objectives: (i) the voltage reference must be designed so as to achieve maximum power point tracking (MPPT), (ii) the DC link voltage must be tightly regulated over a wide range voltage-reference variation, (iii) and the power factor correction (PFC) requirement must be satisfactorily realized. To meet these objectives, a Sliding mode control strategy is applied, based on the nonlinear system model. Then, it is formally demonstrated that the proposed controller actually meets the desired control objectives.

Keywords— three-level neutral point clamped inverter (NPC); grid connected photovoltaic; MPPT; sliding mode; DC voltage constant; Sliding mode control

I. INTRODUCTION

WITH a spurt in the use of renewable energy sources, photovoltaic (PV) power generation is being employed in many applications. Conventionally, a PV system consists of solar PV array and electric converters. A PV array is formed by series/parallel combination of solar modules [1].

Higher power equipment's require higher voltages, which limit the maximum DC voltage level. Therefore a new family

of multilevel inverters has emerged as the solution for solar applications, as the PV array is directly connected to each level of the DC link. Different types of topologies are presented in the literature [2, 3]. This paper uses the NPC topology since it has the advantages such as: (i) DC-link capacitors are common to three phases. (ii) Switching frequency can be low and (iii) reactive current and negative phase sequence current can be controlled.

Several methods of modulation techniques such as selective harmonic elimination PWM, sinusoidal PWM, space vector modulation, sigma delta PWM, closed loop modulation techniques exist to control the inverter [3].

Furthermore, the increase of average PV system size may lead to new strategies like eliminating the DC-DC converter that is usually placed between the PV array and the inverter, and moving the MPPT to the inverter, resulting in increased simplicity, overall efficiency and a cost reduction [4].

The power produced by PV panels is dependent upon the amount of solar irradiance and temperature. The output power produced by PV panels varies as a function of its operating point because of the inherent nonlinear current voltage relationship of a typical PV cell. Therefore, a Maximum Power Point Tracking (MPPT) algorithm is necessary to extract the maximum power from PV panels under varying atmospheric conditions. Many algorithms have been developed for MPPT of a PV array [5]. Among the MPPT techniques, the perturbation and observation (P&O) method is the most popular because of the simplicity of its control

structure. The P&O method moves the operating point toward the maximum power point by periodically increasing or decreasing the array voltage. This method gives good results when the irradiation does not vary quickly.

In grid-connected PV systems (GCPVs). The generated PV power is fed to the grid by three-level NPC inverter and controlled by Sinusoidal PWM technique, or it supplies the linear and nonlinear loads connected at the ac side. In this structure, DC-capacitor is applied to decouple the generators and grid. The converter is used to control the transit power in order to keep the DC-link voltage constant. The control strategy used in this work is field oriented control (FOC) [6].

However, the controller should accommodate the effects of uncertainties and keep the system stable under variable temperature and insulation conditions. The conventional PI-based controllers cannot fully satisfy stability and performance requirements. On the other hand, the system is highly nonlinear and has a large range of operating points. Thus, linearization around one operating point cannot be employed to design the controller. Nonlinear control methods can be used to effectively solve this problem [7].

To control the Grid Connected Photovoltaic Conversion System (GPVCS) we need robust controller. Sliding Mode Control (SMC) is a nonlinear control technique derived from variable structure control system theory and developed by Vladim UTKIN. Such control solution has several advantages such as simple implementation, robustness and good dynamical response. Moreover, such control complies with the nonlinear characteristic of the switch mode power supplies [8].

The remainder of the paper is organized as follows: the next section discusses about the systems configuration, the PV array modeling and its characteristics are described in section-III. Section IV presents an overview and application of P&O algorithm. This is followed by the MPPT structure of the proposed work. In section-V, the modeling converter is described along with the control strategy by sliding mode controller and the simulation results are described in section-VI. Finally, the conclusions are given in the last section.

II. SYSTEMS CONFIGURATION

The proposed system consists of a PV array connected to the three phase three-level NPC through a DC bus which is connected to an ideal grid as shown in Fig. 1.

The control structure of the grid-connected PV system is composed of two structure control.

Control the active and regulate the reactive power injected into the grid;

- A. The MPPT control, whose main property is to extract the maximum power from the PV generator.
- B. The inverter control.
 - To control the active and regulate the reactive power injected into the grid.
 - To control the DC bus voltage.

- To ensure high quality of the injected power. [9];

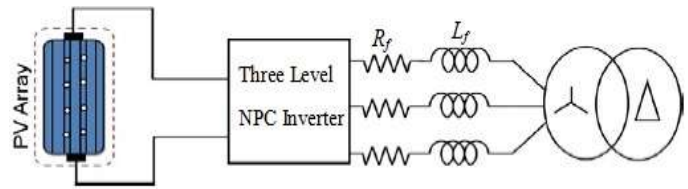


Fig. 1. General diagram of grid connected photovoltaic system

III. MODELING OF PV ARRAY

The basic criteria for modeling a PV device are its electrical characteristics, i.e., the current and voltage-current relationship of a PV cell for varying weather conditions.

A solar PV array is developed in Simulink. This array is used as a source for the maximum power point tracker system. The PV array makes use of the equations of a typical solar cell.

The typical model of a solar cell is shown in Fig. 2. The current and voltage of the solar cell is given as follows:

$$I_{cell} = I_{PV} - I_d - \frac{V_{cell} + R_s I_{cell}}{R_p} \quad (1)$$

$$I_D = I_{sat} \left\{ \exp \left[\frac{q}{kT} (V_{cell} + R_s I_{cell}) \right] - 1 \right\} \quad (2)$$

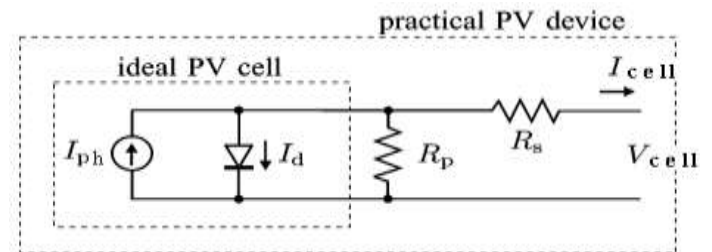


Fig. 2. Solar cell electrically equivalent circuit

Where I_{cell} and V_{cell} are the cell output current and voltage. The definitions of the parameters are given in Table I.

The equivalent circuit for the solar cells arranged in N_p parallel and N_s series is shown in Fig. 3, array current and array voltage becomes:

$$I_{ph} = N_p I_{ph} - N_s I_{sat} \left\{ \exp \left[\frac{q}{kT} \left(\frac{V_{pv}}{N_s} + \frac{R_s I_{pv}}{N_p} \right) \right] - 1 \right\} - \frac{N_p}{R_p} \left(\frac{V_{pv}}{N_s} + \frac{R_s I_{pv}}{N_p} \right) \quad (3)$$

Where N_p represents the number of parallel modules. Note that each module is composed of N_s cells connected in series. $N_p I_{ph}$ corresponds to the short circuit current of the solar array.

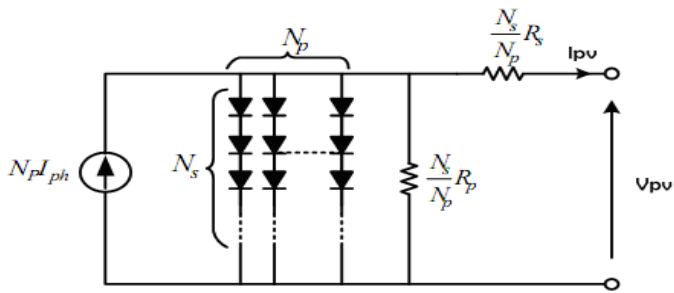


Fig. 3. Electrically equivalent of solar array circuit (N_p parallel - N_s series)

The output of Simulink model is shown first the V-P characteristics of PV module, for various irradiation levels Fig. 4, and then V-I characteristics, reference to the key specifications of the NA-901 module illustrated in Table I, the results of Simulink PV module show the excellent correspondence to the model.

IV. MPPT ALGORITHM

Maximum power point tracking (MPPT) have already been mentioned in Introduction, it is necessary to draw the maximum amount of power from the PV module. We have chosen to use perturb and observe (P&O) algorithm, based on the references mentioned before. Also known as the “hill climbing” method, P&O algorithm is very popular because of its simplicity and ease of implementation. Basically, the module current is perturbed by a small increment, and the resulting change in the power is observed. If the change in power is positive, the current is adjusted by the same increment, and the power is again observed. This continues until the change in power is negative, at which point the direction of the change in current is reversed [10].

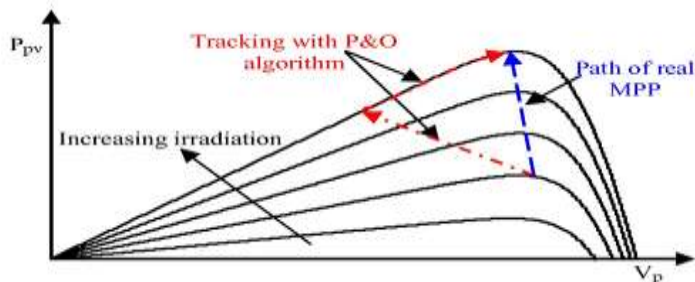


Fig. 4. Deviation from the MPP with the P&O algorithm under rapidly changing irradiance

V. MODELING CONVERTER

The inverter control is based on a decoupled control of the active and reactive power.

A. The Three-Phase Converter

The topology of three-phase three-level NPC grid connected inverter is shown in Fig. 8:

Where, v_{ag}, v_{bg}, v_{cg} are the three-phase symmetrical grid voltage, i_{ag}, i_{bg}, i_{cg} are the three-phase AC grid current, R_f, L_f are the equivalent resistance and inductance of the power grid side, respectively, U_{dc1}, U_{dc2} represent the voltage value of DC bus capacitor C_1, C_2 , U_{dc} is the DC bus voltage. U_{oN} is the voltage of node o referring to neutral point N.

The switching function s_i ($i=a, b, c$) is defined as follows: if s_{i1}, s_{i2} switch on, s_{i3}, s_{i4} switch off, $s_i = 1$, if s_{i2}, s_{i3} switch on, s_{i1}, s_{i4} switch off, $s_i = 0$, if s_{i3}, s_{i4} switch on, s_{i1}, s_{i2} switch off, $s_i = -1$. In the steady state, U_{dc1}, U_{dc2} is almost equal, that is $U_{dc1} = U_{dc2} = U_{dc} / 2$.

Phase voltages of the inverter according to switch position are given in the following equation:

$$\begin{aligned} v_{an} &= \frac{U_{dc1}}{3}(2s_{a1} - s_{b1} - s_{c1}) + \frac{U_{dc2}}{3}(2s_{a2} - s_{b2} - s_{c2}) \\ v_{bn} &= \frac{U_{dc1}}{3}(2s_{b1} - s_{a1} - s_{c1}) + \frac{U_{dc2}}{3}(2s_{b2} - s_{a2} - s_{c2}) \\ v_{cn} &= \frac{U_{dc1}}{3}(2s_{c1} - s_{b1} - s_{a1}) + \frac{U_{dc2}}{3}(2s_{c2} - s_{b2} - s_{a2}) \end{aligned} \quad (4)$$

In this inverter circuit, the gating signals of the inverter switches are generated by using a sinusoidal reference wave modulated with two triangular carrier waves with the same frequency but with opposite offset value. This strategy is able to perform the sinusoidal PWM of the inverter as shown in Fig. 5.

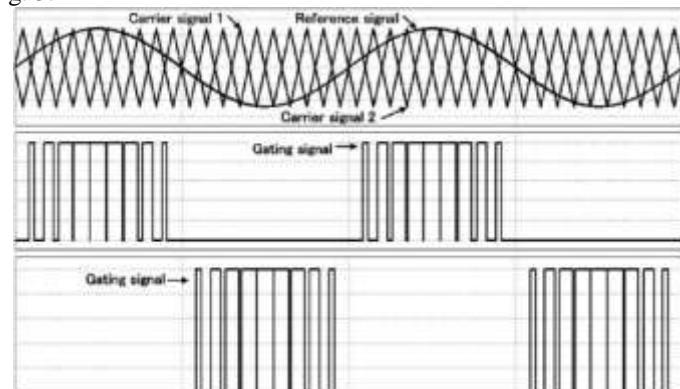


Fig. 5. Sinusoidal PWM for gating signals generation of three-level inverter

In general, modulation index (M) for n level multilevel inverter is given in the following equation:

$$M = \frac{A_m}{(n-1)A_c} \quad (5)$$

Where A_m is the maximum value of reference voltage (V_{ref}) and A_c is the peak to peak value of triangle wave (V_c).

This modulation is a widely extended modulation technique among voltage sourced converters. By using a triangular signal and comparing it with the reference signal (an image of the output voltage that is wanted at the output of the converter), it creates the output voltage according to the following law [11]:

$$S_j = 1 \text{ if } V_j^* > v_{tri} \text{ with } j = a, b, c \quad (6)$$

Where

v_a^*, v_b^*, v_c^* = Reference voltages for each phase
 v_{tri} = Triangular signal

B. Current Control Modeling

The vector current control in Park reference frame is carried out by using the synchronized reference with the grid voltage Fig. 6.

In the synchronous d-q reference frame, the voltage equations, the active power and reactive power equations in the steady state of a three-phase grid-connected PV can be described as (7) and (8) [12].

$$\begin{cases} v_d = R_f i_d + L_f \frac{di_d}{dt} - \omega_s L_f i_q + v_{dg} \\ v_q = R_f i_q + L_f \frac{di_q}{dt} + \omega_s L_f i_d + v_{qg} \end{cases} \quad (7)$$

$$\begin{cases} P = v_{dg} i_d + v_{qg} i_q \\ Q = v_{qg} i_d - v_{dg} i_q \end{cases} \quad (8)$$

If the three-phase grid voltage is ideally sinusoidal without any harmonics, then in the d, q frame, the grid voltage vector is given by

$$\begin{cases} v_{dg} = v_d \\ v_{qg} = 0 \end{cases} \quad (9)$$

In practice, the grid voltage is no sinusoidal due to harmonics. Therefore, both v_d and v_q will not be constant but have slight ripples whose frequencies and magnitudes depend on the harmonic components. However, in steady state, the average value of v_q is still equal to zero.

Consequently, (8) can be rewritten as (10). Its active power depends on the d-axis current, and the reactive power depends on the q-axis current. Furthermore, in order to achieve unity power factor fundamental current flow, the q component of the command current vector is set to zero.

$$\begin{cases} P = v_{dg} i_d \\ Q = -v_{dg} i_q \end{cases} \quad (10)$$

Assuming lossless power transmission between solar array and grid line, the relationship of instantaneous active power exchanged between the PV array and the grid is given by

$$P_{pv} = P = v_d i_d \quad (11)$$

This allows one to obtain the relation

$$i_d = \frac{P_{pv}}{v_d} \quad (12)$$

Therefore, the PV power information can be obtained from the d-axis grid current component by the relation (12).

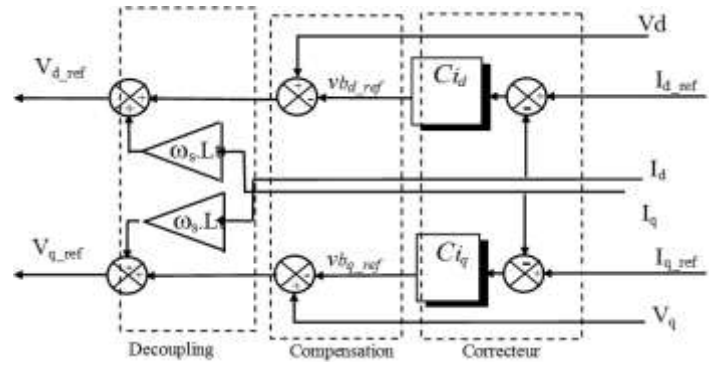


Fig. 6. Bloc diagram of the current control

L_f is the filter inductance, and R_f is the resistance associated both the inverter output side and grid side inductances [13].

C. Voltage Control Modeling

The DC reference voltage v_{ref} is compared with the sensed DC voltage across the capacitor v_{dc} . The DC voltage corrector regulates the DC bus and sets the active power P_{c_ref} which is necessary to charge the capacitor to the desired value. The reference active power P is obtained after being added to the P_{c_ref} the power generated by the PV (P_{MPP}). Fig. 7 shows the bloc diagram of DC voltage control [14].

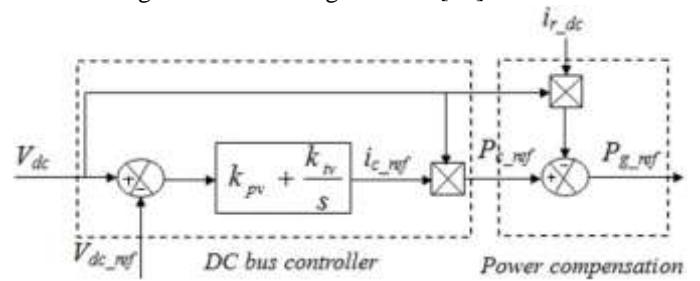


Fig. 7. Bloc diagram of the DC bus control

The instantaneous change indirect bus voltage v_{dc} is given by the capacitive current i_c integration.

$$U_{dc} = \int \frac{1}{C} i_c dt \quad (13)$$

With:

$$i_c = i_{dc} - i_g \quad (14)$$

And

$$i_g = F_1 i_{ag} + F_2 i_{bg} + F_3 i_{cg} \quad (15)$$

F_1, F_2, F_3 are logic functions according to the switch states given by the grid link control and i_{ag}, i_{bg}, i_{cg} , are the three phase currents supplied to the grid.

D. Sliding Mode Control

The SM controller has been very successful in recent years due to the simplicity of its implementation and its robustness against the uncertainties of the system and external disturbances in the process. Sliding mode control is to bring

back the state trajectory to the sliding surface and to advance on it with a certain dynamic point balance [15].

1) Control Design

The two switching surfaces and are defined by:

$$\begin{cases} S_1 = i_{d_ref} - i_d \\ S_2 = i_{q_ref} - i_q \end{cases} \quad (16)$$

So:

$$\begin{cases} \dot{S}_1 = \dot{i}_{d_ref} - \dot{i}_d \\ \dot{S}_2 = \dot{i}_{q_ref} - \dot{i}_q \end{cases} \quad (17)$$

When the sliding mode occurs on the sliding surface, then:

$$S_1 = \dot{S}_1 = S_2 = \dot{S}_2 = 0 \quad (18)$$

To satisfy the stability equation and to get a sliding mode control, a possible control variable can be given as:

$$\begin{cases} v_{d_ref} = v_{eq_d} + v_{n_d} \\ v_{q_ref} = v_{eq_q} + v_{n_q} \end{cases} \quad (19)$$

Combing (7), (16), (17), (18) and (19) the controls voltage of d-q axis is defined by:

$$\begin{cases} v_{eq_d} = R_f i_d - L_f \omega i_q + v_g \\ v_{n_d} = K_d \text{sign}(S_1) \end{cases} \quad (20)$$

$$\begin{cases} v_{eq_q} = R_f i_q - L_f \omega i_d \\ v_{n_q} = K_q \text{sign}(S_2) \end{cases} \quad (21)$$

Where $K_d > 0$ and $K_q > 0$

By the development of eq. (10) we write the eq. (22).

The GSC output currents set value are deduced as:

$$\begin{cases} i_{d_ref} = \frac{P}{v_{dg}} \\ i_{q_ref} = -\frac{Q}{v_{dq}} \end{cases} \quad (22)$$

VI. SIMULATION RESULTS, DISCUSSION AND COMPARISON

Computer simulation has been done using MATLAB/Simulink in order to validate the performance of the proposed control strategy are described in Fig. 8. For all simulations, The PV system of 5.6 kW maximal is developed using 5 parallel connected strings with each string having 13 series connected PV modules. The parameters of the PV system and electrical power system that are used in simulation are given in Table-I. The dc-link capacitors are 1100 μF each, and the AC filter has an inductance of 37 mH; the switching frequency is fixed at 10 kHz.

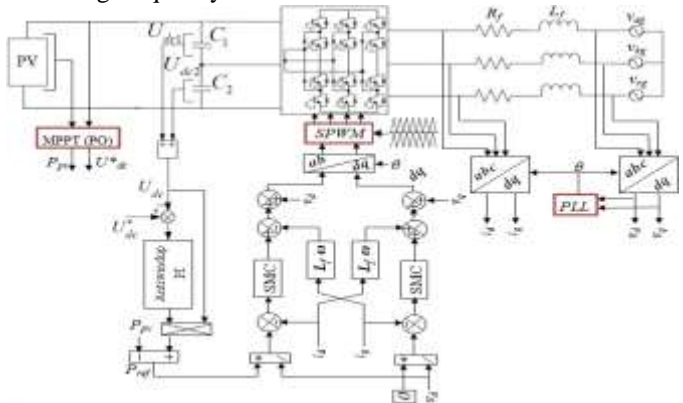


Fig. 8. System control structure diagram

A. Simulation under constant atmospheric conditions

Simulation results under two atmospheric conditions, temperature 25°C and irradiance 1000 W/m², are presented in Figs. 9.

As can be seen from these figures, the MPPT controller quickly adjusts voltage references in order to track the maximum power point.

The power active and reactive follows quietly those references respectively as shown in Fig. 9(c).

As shown in Fig. 9(d), in the steady state, the grid current and grid voltage satisfy the unit-power-factor condition. From the grid current spectrum diagram in Fig. 10, the sliding mode controller has good performance in harmonic compensation, and the current total harmonic distortion (THD) is as low as 1.96%.

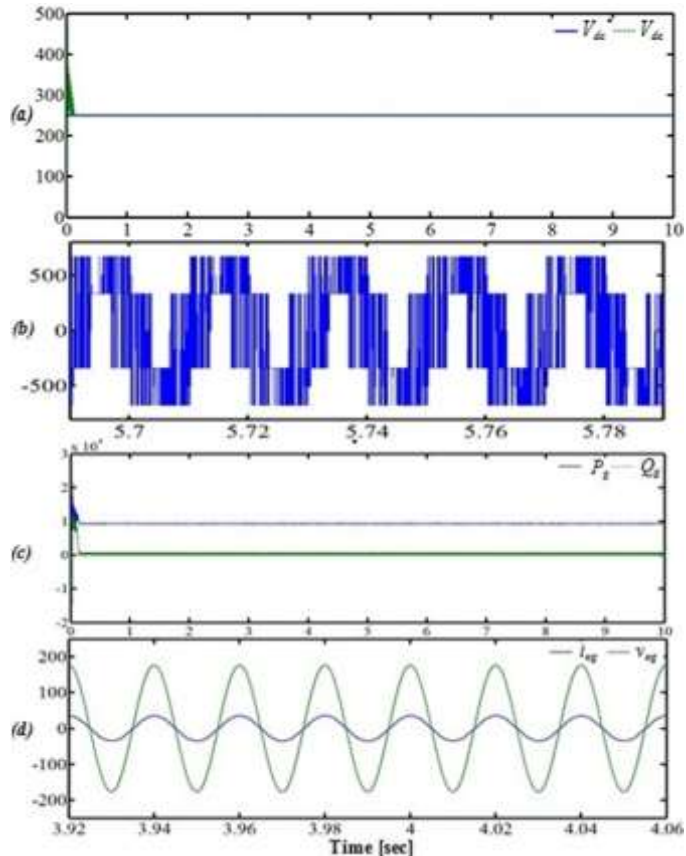


Fig. 9. Simulation results under constant atmospheric conditions. (a) DC-link capacitor voltages ([V]). (b) Voltage for a three-level NPC inverter ([V]). (c) Active and reactive grid power ([W], [VAR]). (d) Phase a current and voltage ([A], [V]).

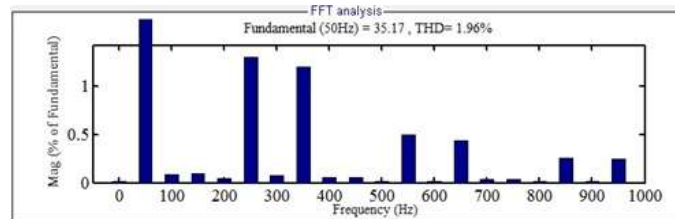


Fig. 10. THD analysis of phase a grid current.

B. Simulation under changing atmospheric conditions

In this section, a rapid increase in irradiance from 400W/m² to 1000W/m² within a time period of 2 seconds and a change back to 400 W/m² at t = 6.5s was simulated . The cell temperature was kept at a constant value of 25°C. The obtained results are presented in Figs. 11. These results show a good robustness of the proposed controller with respect to irradiation variations.

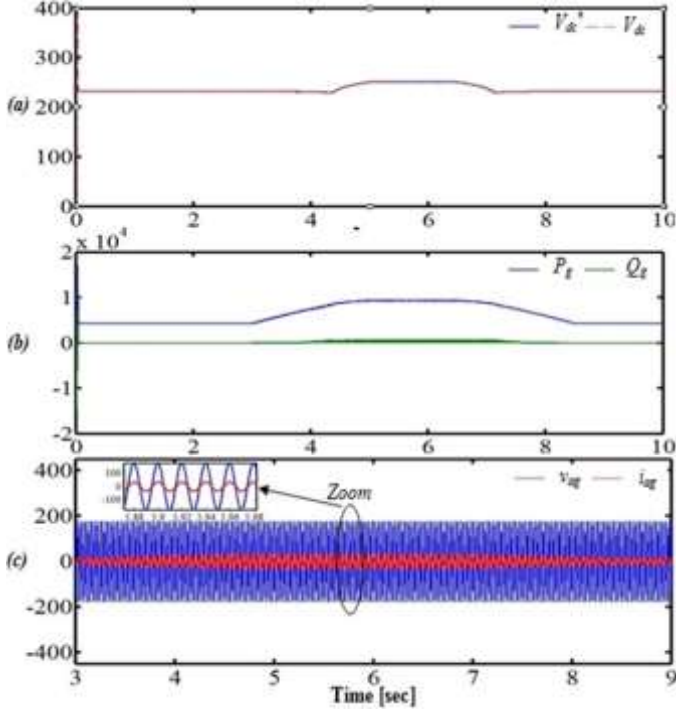


Fig. 11. Simulation results under changing atmospheric conditions. (a) DC-link capacitor voltages ([V]). (b) Active and reactive grid power ([W], [VAR]). (c) Phase a current and voltage ([A], [V]).

VII. CONCLUSION

In this paper, a nonlinear control of NPC three-level photovoltaic grid-connected inverter is proposed. the use of a three level NPC with his simplified control algorithm (SPWM) as a grid interface gives a good results in term of THD and power quality, also, the aim was in this work to inject to the grid a maximum power possible whatever solar irradiance and temperature condition. The proposed control laws are derived from the Lyapunov approach using sliding mode controllers. This sliding mode control strategy has been adopted to obtain better dynamic performances. The simulation results included in the paper, indicate that the unity power factor is achieved and the proposed SMC scheme exhibits better steady state performance and can reduce the three-level inverter voltage fluctuation significantly compared to the conventional PI controller.

APPENDIX

TABLE I. ELECTRICAL CHARACTERISTIC OF PV PANEL WITH AN IRRADIANCE LEVEL OF 1000 W/M²

Symbol	Quantity
STP 080	Model
12/Bb	
$V_{oc}=21.9V$	Open voltage
$V_{mp}=17.5V$	Optimal voltage
$I_{sc}=4.95A$	Short-circuit current
$I_{mp}=4.57A$	Optimal current
$P_m=80W$	Maximal Power
-40° C a	Operating temperature
85° C	
1195×541×	Dimensions
30 (mm)	
8 kg	Weight

^aGaussian units are the same as cgs emu for magnetostatics; V = volt, A = ampere, T = temperature, mm = millimeter, kg = kilogram

ACKNOWLEDGMENT

The authors would like to acknowledge the financial support of the Algeria's Ministry of Higher Education and Scientific Research.

REFERENCES

- [1] Kun Ding, XinGao Bian, HaiHao Liu, and Tao Peng, "A MATLAB-Simulink-Based PV Module Model and Its Application Under Conditions of Nonuniform Irradiance", IEEE Trans. ENERGY CONVERSION, VOL. 27, NO. 4, DECEMBER 2012.
- [2] J. Rodriguez, J.S. Lai, F.Z. Peng, "Multilevel inverters: a survey of topologies, controls, and applications", IEEE Transactions on Industrial Electronics 2002, 49 (4), 724–738.
- [3] I. Colak, E. Kabalci, R. Bayindir, "Review of multilevel voltage source inverter topologies and control schemes", Energy Conversion and Management 2011, 52 (2), 1114–1128.
- [4] Jaime Alonso-Martínez, Santiago Arnaltes, "A Three-Phase Grid-Connected Inverter for Photovoltaic Applications Using Fuzzy MPPT", International Conference on Renewable Energy, 2009.
- [5] R. Kadri, Jean-Paul Gaubert, and Gerard Champenois, "An Improved Maximum Power Point Tracking for Photovoltaic Grid-Connected Inverter Based on Voltage-Oriented Control", IEEE Transactions On Industrial Electronics, Vol. 58, No. 1, January 2011.
- [6] M. Emna, Adel Khedher, M.Faouzi, The Wind energy Conversion System Using PMSG Controlled by Vector Control and SMC Strategies, International Journal Of Renewable Energy Research, Vol.3, No.1, 2013.
- [7] N. Khemiri, A. Khedher, M.F. Mimouni, "Wind Energy Conversion System using DFIG Controlled by Backstepping and Sliding Mode Strategies", International Journal Of Renewable Energy Research, Vol.2, No.3, 2012.
- [8] A. Tahour, A.G. Aissaoui, M. Abid, N. Essounbouli, F. Nollet, Sliding Mode Control Of Chopper Connecting Wind Turbine With Grid Based On Synchronous Generator, Proceedings of the 2014 International Conference on Power Systems, Energy, Environment.
- [9] F.Bouchafaal, D.Berberl, M.S.Boucherit, "Modeling and simulation of a grid connected PV generation system With MPPT fuzzy logic control," IEEE, 7th International Multi-Conference on Systems, Signals and Devices, vol. 20, pp. 569–571, 2010.

- [10] F.Z. Amatoul, M.T. Lamchich, A. Outzourhit, "Design Control of DC/AC Converter for a grid Connected PV Systems using Matlab/Simulink", Proceedings of the 2011-14th European Conference on Power Electronics and Applications (EPE 2011), pp. 1-7.
- [11] G. Abad, J. Lopez, M. A. Rodriguez, L. Marroyo, G. Iwanski, "Doubly Fed Induction Machine: Modeling And Control For Wind Energy Generation," IEEE Press Editorial Board., TK2451.D68 2011.
- [12] Hui Zhang, Hongwei Zhou, Jing Ren, Weizeng Liu, Shaohua Ruan and Yongjun Gao, Three-Phase Grid-Connected Photovoltaic System with SVPWM Current Controller, IEEE Electron Device Lett., IPERC, 2009.
- [13] R. Teodorescu, M. Liserre, P. Rodriguez, "Grid Converters for Photovoltaic and Wind Power Systems," IEEE Electron Device Lett., TK7872.C8T46 2011.
- [14] T. Ghennam, E.M.Berkouk, B.François, Modeling and Control of a Doubly Fed Induction Generator (DFIG) Based Wind Conversion System, IEEE POWERENG 2009, Lisbon, Portugal, March 18-20, 2009.
- [15] J.J.Slotine, "Adaptive Sliding controller synthesis for nonlinear systems," IJC, Vol 43 .N°6, 1986, pp 1631-1651.